·Experimental Research·

Establishment of a lens opacity model in Grx2 knockout mice based on the CRISPR/cas9 system and the role of Grx2 in cataract pathogenesis

Guo Yong[1], Guo Chenjun[2], Zhang Jie[2], Ning Xiaona[2], Chen Xi[3], Yan Hong[1]

[1]Department of Ophthalmology, Xi'an People's Hospital, Xi'an Fourth Hospital, Shaanxi Eye Hospital, Xi'an 710004, China; [2]Department of Ophthalmology, Tangdu Hospital of Air Force Medical University, Xi'an 710038, China; [3]Department of Ophthalmology, Second Affiliated Hospital of Chongqing Medical University, Chongqing 400010, China

Corresponding author: Yan Hong, Email: yan2128ts@hotmail.com

[Abstract] Objective To investigate the role of glutatedoxin (Grx2) in cataract pathogenesis by establishing *Grx2* knockout (KO) and knockin (KI) mouse models.

Methods Ten black C57BL/6J mice were selected to establish a *Grx2* KO model (*n*=5) and a *Grx2* KI model (*n*=5) using the CRISPR/Cas9 system. The offspring mice were sequenced by tail clipping and included in the corresponding experimental group according to the genotype. The general condition and lens opacity were recorded. After the mice were euthanized, the lens pathological changes were observed by hematoxylin-eosin staining. The reactive oxygen species (ROS) and 8-hydroxy-desoxyguanosine (8-OHdG) contents were analyzed by enzyme-linked immunosorbent assay. The relative Grx2, glutathione (GSH), B-cell lymphoma-2 (bcl-2), glutathione disulfide (GSSG) and bcl-2-associated X protein (bax) expression levels in the lens were assayed.

Results The offspring of *Grx2* KO and *Grx2* KI homozygous and heterozygous mice were confirmed by tail cutting nested polymerase chain reaction and gene sequencing. Compared with the wild type (WT) mice of the same age, the lens opacity of *Grx2* KO heterozygous mice occurred earlier, whereas the lens of *Grx2* KI homozygous mice remained transparent throughout the study. A large number of gaps and vacuoles were found in the lens fibers of 5-month-old *Grx2* KO mice. The lens 8-0HdG content and ROS fluorescence intensity (absorbance, A value)of 5-month-old *Grx2* KO mice were 3.886±0.326 ng/ml and 1594±132, respectively, which were significantly higher than 3.531±0.250 ng/ml and 1157±123, respectively, in WT mice (t=2.711, P=0.033; t=3.384, P=0.028). The relative Grx2, GSH and bcl-2 expression levels in the lens of 5-month-old *Grx2* KO mice were 0.23±0.01, 0.70±0.06 and 0.32±0.03, respectively, which were significantly lower than 0.52±0.02, 1.04±0.08 and 0.49±0.04, respectively, of WT mice (t=2.815, P=0.020; t=2.457, P=0.033; t=2.279, P=0.041).

Conclusions *Grx2* KO and *Grx2* KI mouse models were successfully established in this study. The occurrence and development of age-related cataract were accelerated in *Grx2* KO mice.

[Key words] Cataract; Oxidative damage; Glutaredoxins; Gene knockout techniques; Gene knock-in techniques; Mice; Lens epithelial cells

Fund program: National Natural Science Foundation of China (81570823)

DOI: 10. 3760/ema.j.cn115989-20210308-00149

A variety of endogenous and exogenous factors, including aging, radiation, genetics, toxicity, trauma, immunity and local metabolic and nutritional disorders, can induce cataracts. Cataract has many causative factors and its pathogenesis remains unclear. Oxidative stress and free radical injury are common pathways by which various factors contribute to cataract occurrence[1]. As verified recently, there are multiple antioxidant defense lines within healthy lens epithelial cells (LECs). Free radicals generated by causative factors will be cleared by the first line of defense (i.e., antioxidants and antioxidant enzymes) in the lens. When antioxidant enzymes are depleted, the second line of defense (i.e., the antioxidant enzyme repair system) will be activated. The second line of defense consists mainly of the thioltransferase/glutaredoxins (TTase/Grxs) and thioredoxin/thioredoxin reductase dynamic systems, which reestablishes the oxidation/antioxidation dynamic balance of the lens by controlling the thiol/disulfide content [2]. TTase/Grx exists in two isoforms, namely Grx1 is distributed in the cytoplasm and Grx2 in the mitochondrion and nucleus. As isozymes, Grx1 and Grx2 can both undergo desulfurization, and repair antioxidant enzymes and antioxidants, thereby maintaining the antioxidant dynamic balance [3-4]. Grx2 is important for scavenging free radicals, repairing LECs, protecting LEC activity and preventing cataract formation [5]. However, there remains a lack of evidence regarding the effect of Grx2 inhibition on lens opacity at the tissue and bodily levels. In this study, *Grx2* knockout (KO) and knockin (KI) mouse models were established by the clustered regularly interspaced short palindromic repeats/CRISPR-associated 9 (CRISPR/Cas9) system to observe the occurrence and development of lens opacity in mice and to investigate the role of *Grx2* gene in cataractogenesis, aiming to provide new ideas for research on anti-cataract drugs.

1 Materials and Methods

1.1 Materials

1.1.1 Laboratory animals Ten black C57BL/6J male mice of clean grade (provided by the Laboratory Animal Center of the Second Affiliated Hospital of Chongqing Medical University, China) were equally divided into two groups for *Grx2* KO and KI, respectively. They were housed in a laminar flow clean room with lighting from 6:00 to 18:00 and a room temperature of 20°C, and provided with sterile drinking water, feed and dressings. The laboratory animals and housing environment met the national standard *Laboratory animal - Requirements of environment and housing facilities* (GB14925). The use and feeding of laboratory animals were in accordance with the Regulations on the Administration of Laboratory Animals issued by the State Science and Technology Commission. The study protocol was approved by the Ethics Committee of the Second Affiliated Hospital of Chongqing Medical University [approval No.: 2020 KLS (125)].

1.1.2 Main reagents and instruments The following reagents

and instruments were used: REDExtract-N-Amp Tissue polymerase chain reaction (PCR) kit (Sigma, Santa Clara, CA,USA), bicinchoninic acid (BCA) protein assay kit (Pierce, USA), mouse anti-Grx2 (ab167207) and mouse anti-glutathione (GSH) monoclonal antibodies (ab19534) (both, Abcam, USA), rabbit anti-glutathione disulfide (GSSG) polyclonal antibody (AB5010, Sigma-Aldrich, USA), β-actin (GB11001), horseradish peroxidase -labeled goat anti-mouse (G1214) and goat anti-rabbit secondary antibodies (G1213) (all Servicebio, Wuhan, China), rabbit B-cell lymphoma-2 (bcl-2) polyclonal antibody (26593-1-AP) and rabbit bcl-2-associated X protein (bax) polyclonal antibody (50599-2-Ig) (both Proteintech, Wuhan, China), 2',7'-Dichlorofluorescin diacetate (DCFH-DA) (Shanghai Beyotime Biotechnology Co., Ltd., China), reactive oxygen species (ROS) enzyme-linked immunosorbent assay (ELISA) kit (Shanghai Enzyme-linked Biotechnology Co., Ltd., Shanghai, China), 8-hydroxy-desoxyguanosine (8-OHdG) ELISA kit (Elabscience Biotechnology, Wuhan, China), PCR instrument (Bio-Rad, USA), slit-lamp microscope (SL130, Carl Zeiss, Germany), light microscope (CKX53, Olympus, Japan), fluorescence spectrophotometer (Epoch, USA) and enhanced chemiluminescence (ECL) Western blotting system (Thermo Fisher Scientific, USA).

1.2 Methods

1.2.1 Establishment of the *Grx2* KO mouse model The *Grx2* gene was knocked out using the CRISPR/Cas9 system [6] with reference to the literature [7], specifically as follows: (1) Vector design and construction: this included the design of a small guide RNA (sgRNA) recognition sequence, the construction of an sgRNA plasmid and verification by sequencing. (2) *In vitro* transcription: this included Cas9 extraction and purification and *in vitro* sgRNA transcription and purification. (3) Pronuclear injection: this included superovulation of mice and transplantation after fertilized egg injection, thereby obtaining F0-generation mice. (4) Mouse gene identification: this included the verification of *Grx2* KO mice by PCR and sequencing, and the identification of mutation sequence by further sequencing.

1.2.2 Establishment of the *Grx2* KI mouse model The *Grx2* gene was inserted into the target strand at a specific position using the CRISPR/Cas9 system and homologous recombination vector (donor vector), specifically as follows: (1) Preparation of guide RNA (gRNA) and Donor vector: the plasmid required for the CRISPR/Cas9 system was prepared, and gRNA was designed, followed by *in vitro* transcription in mice, thereby obtaining the Donor vector. (2) Fertilized egg injection in mice: fertilized eggs were obtained by *in vitro* fertilization and microinjected with the prepared gRNA, donor vector and Cas9 protein. (3)CRISPR/Cas9 system activation in the fertilized egg: gRNA was used for guidance, Cas9 for cleaving at the specific site of double-stranded DNA and donor vector for inserting the *Grx2* gene and repairing double-stranded DNA [8].

1.2.3 Breeding and sequencing of mice Heterozygous C57BL/6J-*Grx2* KO and C57BL/6J-*Grx2* KI mice were housed in a laminar flow clean room and provided separately with sterile water, food and padding. Their toes were clipped and labeled, with forelimbs as the tens digit and hindlimbs as the units digit. Following the estrus period at one month of age, one male and one female were selected for natural mating and breeding. After breeding expansion in five isolated cages, the mice were used for later experiments. Following a gestation period of approximately 20 days, female mice gave birth to offspring, which were housed in separate cages after 1 week of age and had good development status. Subsequently, gene sequencing was performed using the REDExtract-N-Amp Tissue PCR kit. The genotype was recorded as KO-KO for homozygous *Grx2* KO micewhen the *Grx2* gene sequence was deleted in the two DNA strands. Similarly, the genotype was recorded as WT-WT for wild-type mice, KO-WT for heterozygous *Grx2* KO mice, KI-KI for homozygous *Grx2* KI mice and KI-WT for heterozygous *Grx2* KI mice.

1.2.4 Observation of lens opacity in mice under a slit-lamp microscope Lens opacity in *Grx2* KO, *Grx2* KI and C57BL/6J WT mice was observed under the slit-lamp microscope weekly until aged 5 months. The pupil of mice was fully dilated with topical tropicamide (0.5%) and phenylephrine hydrochloride eye drops (0.5%) three times (5 min/time). After 15 min, the lens was observed from the front with a slit light source of the slit-lamp microscope under an angle of incidence of 15°, and the site and degree of lens opacity were recorded. The mouse lens was graded with reference to the Oxford Clinical Cataract Classification and Grading System [9]. Grade 0: the lens was completely transparent; Grade 1: the lens was transparent but with scattered vacuoles in the cortex; Grade 2: the lens had a mild increase in nuclear density, lens capsular opacity emerged and more vacuoles appeared in the cortex; Grade 3: the lens had an increase in nuclear density and white lamellar opacity in the cortex; Grade 4: the entire lens displayed white opacity.

1.2.5 Observation of histopathological changes in mouse lens, heart, brain, liver and muscle by hematoxylin-eosin (HE) staining At the nineteenth month of feeding, the mice were euthanized with CO_2. The eyeballs were enucleated and scissored from the equator using a dissecting microscope and ophthalmic microsurgical instruments, from which the lens was peeled off completely without damaging the lens capsule. The lens weight was determined immediately using an electronic balance. Five lenses were randomly selected, placed into a plastic embedding cassette containing 4% paraformaldehyde, labeled and stored, followed by HE staining. The remaining lenses were freeze-dried on dry ice and stored at 80°C for later use. Following eyeball enucleation, the mice were dissected with ophthalmic scissors, and the metabolically active tissues such as the heart, brain, liver and muscle were harvested. The tissues were cut into pieces (5 mm × 5 mm × 2 mm) with ophthalmic scissors, immediately placed in a plastic embedding cassette containing 4% paraformaldehyde, labeled and stored, followed by HE staining. The histopathological changes were observed under a light microscope.

1.2.6 Mouse lens ROS and 8-OHdG levels determined by ELISA The lenses stored at −80°C was lysed and homogenized, and the supernatant was harvested. Subsequently, the lens ROS and 8-OHdG contents were determined using a fluorescence spectrophotometer in accordance with the instructions of the ROS and 8-OHdG ELISA kits.

1.2.7 Measurement of relative protein expressions of oxidative stress-related indicators in mouse lens by Western blotting The protein was extracted from the lenses and its concentration determined by the BCA assay. Subsequently, an equal amount of protein of oxidative stress-related indicators was subjected to 12% sodium lauryl sulfate polyacrylamide gel electrophoresis (SDS-PAGE) and transferred onto a (PVDF) membrane, followed by incubation with primary antibodies (1:1000) against *Grx2*, GSH, Bcl-2, GSSG, Bax and β-actin at 4°C for 8 h

and with the corresponding secondary antibodies (1:4000) at room temperature for 2 hours. Following ECL Western blotting, the image grayscale values of Grx2, GSH, bcl-2 and bax were analyzed using Image J, based on which the relative protein expression levels were detected, with β-actin as an internal reference.

1.3 Statistical methods

SPSS 19.0 software was used for statistical analysis. Measurement data were verified by Shapiro-Wilk test to be normally distributed and described by ($\bar{x}\pm s$). Lens weight was compared by one-way analysis of variance among *Grx2* KO, *Grx2* KI and WT mice of the same month of age, and the 8-OHdG and ROS contents and the relative Grx2, bcl-2, GSH, GSSG and bax protein expression in the lens were compared by independent-samples *t*-test between *Grx2* KO and WT mice. A $P<0.05$ was considered to be statistically significant.

2 Results

2.1 Gene sequencing results of the *Grx2* KO mice

The DNA electrophoresis results of the F1-generation mice (18#–31#) showed that a 580 bp band and an 883 bp band were amplified in KO-WT mice 26#, 28#, 30# and 31# (Figure 1). The electrophoresis results of F2-generation *Grx2* KO mice showed that a 580 bp band was amplified in KO-KO mice, an 883 bp band in WT-WT mice and both, a 580 bp band and an 883 bp band in KO-WT mice (Figure 2).

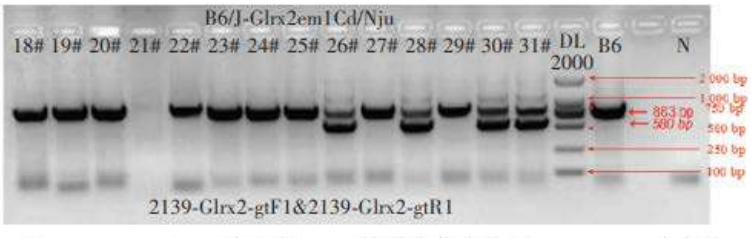

Figure 1 PCR amplification electrophoretogram of *Grx2* Ko F1 mice gene A 580 bp and an 883 bp fragments were displayed. The numerals were mouse tail marking serial number. B6: negative control N: blank control

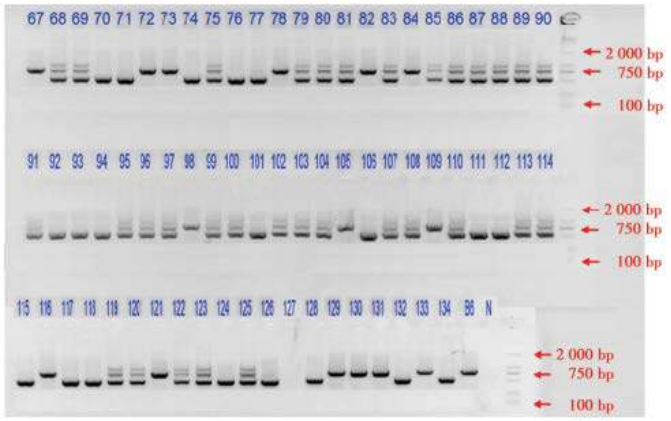

Figure 2 PCR amplification electrophoretogram of *Grx2* KO F2 mice gene A 580 bp fragment was amplified in KO-KO mice, an 883 bp fragment was displayed in WT-WT mice, and both 580 bp and 883 bp fragments were displayed in KO-WT mice. The numerals were mouse tail marking serial number. B6: negative control N: blank control

2.2 Gene sequencing results of the *Grx2* KI mice

According to the PCR gene amplification and sequencing results of *Grx2* KI mice, the mice 110#, 113#, 114#, 115# and 118# were homozygous F2-generation mice (KI-KI) (Figure 3).

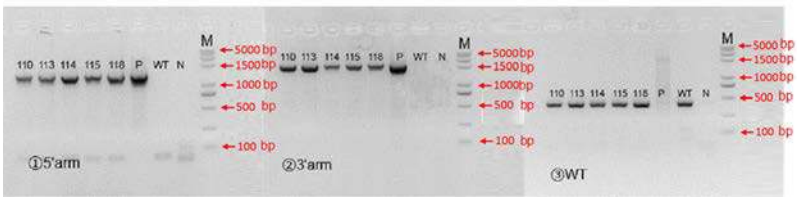

Figure 3 PCR electrophoretogram of *Grx2* KI F2 mice gene sequance A 1 465 bp and a 2 292 bp fragments were displayed from the KI-K1 mouse, a 412 bp fragment was amplified from the WT-WT mouse, and all the fragments were amplified from the KO-WT mouse The numerals were mouse tail marking serial number. P: positive control; WT: wild-type C57BL/6J mouse; N: blank control; M: DNA macular marker; 5' arm: 5' terminal of the gene; 3 'arm: 3' terminal of the gene; WT: wild-type

2.3 General conditions of the mice

Grx2 KO and *Grx2* KI mice were bred and the number of their offspring is shown in Table 1. *Grx2* KO, *Grx2* KI and WT mice were all in good condition and similar in size, habit, body mass, and growth and development status. At 1–19 months of age, there was no statistically significant difference in the lens weight among the *Grx2* KO, *Grx2* KI and WT mice of the same month of age ($P > 0.05$) (Figure 4).

Table 1 Offspring number of different genotype of mice (*n*)

Generation	Offspring number of different genotype			
	KO-KO	KO-WT	KI-KI	KI-WT
F0	0	1	0	1
F1	0	4	0	2
F2	20	32	5	7
F3	32	14	18	23
F4	68	11	20	96

Note: KO: knockout; KI: knockin; WT: wild type

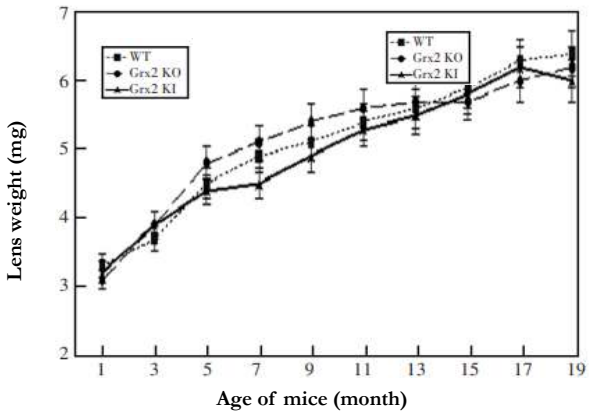

Figure 4 Comparison of lens weight at the same age among different genotype mouse No significant differences were found in lens weight at the same age among different genotype mouse (all at $P>0.05$) (One way ANOVA) WT: wild type ($N=120$); KO: knockout ($N=136$); KI: knockin ($N=40$)

2.4 Lens conditions of mice with different genotypes

The lens of the *Grx2* KO, *Grx2* KI and WT mice remained transparent during the first two months. When aged 3 months, only a few vacuoles were found around the lens of *Grx2* KO mice. When aged 4 months, the nuclear density began to slightly increase. When aged 5 months, the lens of *Grx2* KO micedisplayed lamellar opacity, while only one mouse showed complete opacity. By contrast, at 5 months, only a few vacuoles were observed around the lens of WT mice. The lenses of *Grx2* KI mice remained transparent at all times (Figure 5, Table 2).

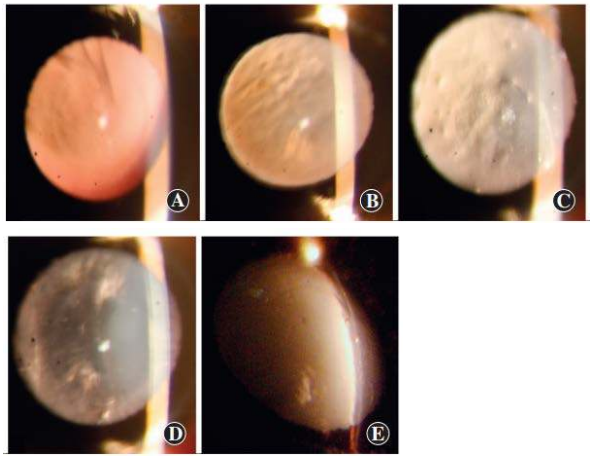

Figure 5 Grading of mouse lens opacity according to Oxford Clinical Cataract Classification and Grading System[9] A: Grade 0 B: Grade 1 C: Grade 2 D: Grade 3 E: Grade 4

Table 2 Comparison of different lens opacity grades among various genotype mice (*M* [*Q1*, *Q3*])

Genotype	*n*	Opacity grading in different age mice				
		1-month old	2-month old	3-month old	4-month old	5-month old
Grx2 KO	40	0(0,0)	0(0,1)	1(0,2)	2(1,3)	3(1,4)
Grx2 KI	40	0(0,0)	0(0,0)	0(0,0)	0(0,0)	0(0,0)
WT	60	0(0,0)	0(0,0)	0(0,1)	1(0,2)	1(0,2)

Note: KO: knockout; KI: knockin; WT: wild type

2.5 Histopathological changes in the lens of mice with different genotypes

It was observed by HE staining that when aged 5 months, the LECs were dark and located in the superficial cortex, and the lens fibers were red and regularly arranged. The results of histopathological staining revealed that *Grx2* KO mice had edema of the lens fibers, with lens fiber breakage and vacuoles and gaps between fibers as compared to *Grx2* KI and WT mice (Figure 6).

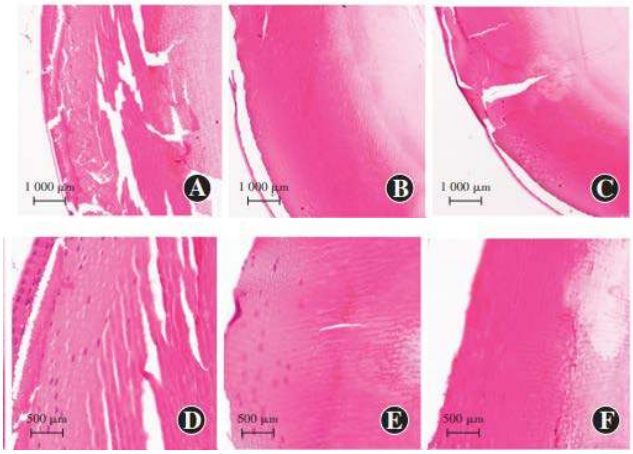

Figure 6 Histopathological changes of lens in various genotype mice (HE) Compared with WT and *Grx2* KI mice, the lens fibers of *Grx2* KO mice appeared fractured and vacuoles A: *Grx2* KO (×100, bar=1 000 μm) B: WT mouse (×100, bar=1 000 μm) C: *Grx2* KI mouse (×100, bar=1 000 μm) D: *Grx2* KO mouse (×200, bar=500 μm) E: WT mouse (×200, bar=500 μm) F: *Grx2* KI mouse (×200, bar=500 μm)

2.6 Histopathological changes in heart, brain, liver and muscle of mice with different genotypes

When aged 5 months, *Grx2* KO and *Grx2* KI mice displayed without significant damage to the heart, brain, liver or muscle. The fibril spaces of heart and muscle were slightly increased, and the tissue gaps of brain and liver were slightly enlarged in *Grx2* KO mice, but had no significant changes compared with that in *Grx2* KI and WT mice (Figure 7).

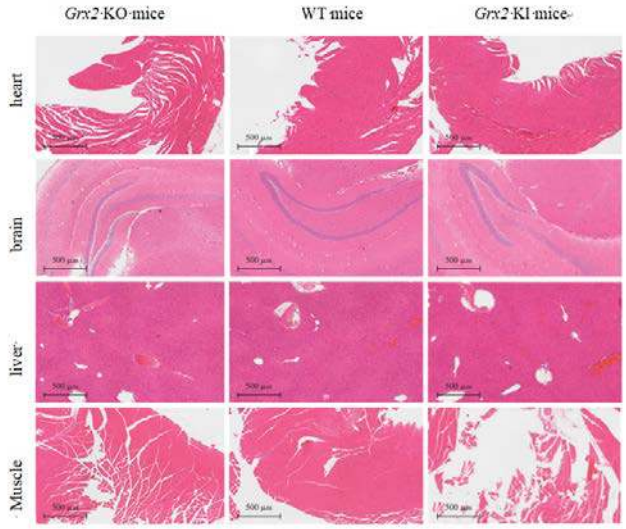

Figure 7 Pathological changes of heart, brain, liver and muscle in different genotype mice When aged 5 months, the heart, brain, liver and muscle tissues were normal. Compared to WT and *Grx2* KI mice, The fibril spaces of heart and muscle were slightly increased, and the tissue gaps of brain and liver were slightly enlarged in *Grx2* KO mice KO: knockout; WT: wild type; KI: knockin

2.7 Comparison of lens 8-OHdG and ROS contents between *Grx2* KO and WT mice

When aged 5 months, the lens 8-OHdG content of *Grx2* KO mice 3.886±0.326 ng/ml was higher than that of the WT mice 3.531±0.250 ng/ml, with the difference being statistically significant (t=2.711, P=0.033) (Figure 8). The ROS fluorescence intensity in the lens of *Grx2* KO mice 1594±132 FI/mg was higher than that of WT mice 1157±123 FI/mg, being statistically significantly different (t=3.384, P=0.028) (Figure 9).

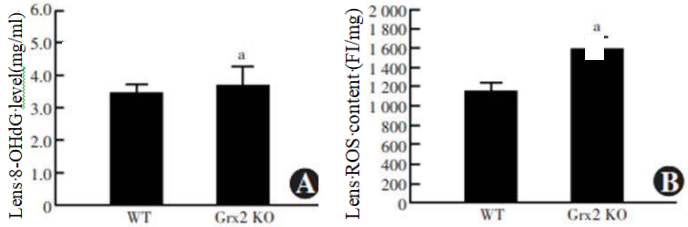

Figure 8 Comparison of lens 8-OHdG and ROS contents between *Grx2* KO and WT mice (Independent samples t test, n=3) Compared with WT mice, $^aP < 0.05$ 8-OHdG: 8-hydroxy-deoxyguanosine; ROS: reactive oxygen species; FI: fluorescence intensity

2.8 Comparison of relative expressions *Grx2*, bcl-2, GSH, GSSG and bax proteins in lens between *Grx2* KO mice and WT mice

When aged 5 months, the relative expressions of *Grx2*, GSH and bcl-2 in the lens of *Grx2* KO mice were lower than those of WT mice (0.23±0.01 *vs.* 0.52±0.02, 0.70±0.06 *vs.* 1.04±0.08 and 0.32±0.03 *vs.* 0.49±0.04, respectively), and the differences were statistically significant (t=2.815, 2.457 and 2.279, respectively, P=0.020, 0.033 and 0.041, respectively). No statistically significant differences were found in the relative expressions of lens GSSG or bax proteins between *Grx2* KO and WT mice (0.34±0.03 *vs.* 0.41±0.03 and 0.16±0.01 *vs.* 0.18±0.01, respectively) (t=0.933 and 0.752, respectively, P>0.05) (Figure 9).

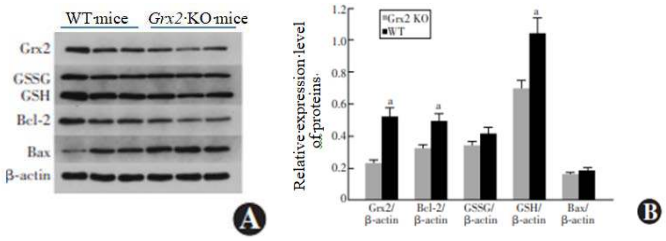

Figure 9 Comparison of lens Grx2, bcl2, GSSG, GSH and bax protein levels between *Grx2* KO and WT mice A: Western blot electrophoretogram B: Comparison of relative expression levels of Grx2, bcl-2, GSSG, GSH and bax Compared with WT mice, $^aP < 0.05$ (Independent samples *t* test, $n=3$) WT: wild type; KO: knockout; GSSG: glutathione disulfide; GSH: glutathione; bcl-2: B cell lymphoma-2 gene; bax: bcl-2-associated X protein

3 Discussion

Grx displays diversity, with three subtypes of Grx2 and two subtypes of Grx3 and Grx5 [10]. Grx2 is widely expressed in human organs and is involved in the second line of cellular antioxidant defense to reestablish the intracellular GSH/GSSG dynamic homeostasis and restore the oxidation/antioxidation stability *in vivo* [11-12]. Under normal physiological conditions, two molecules of Grx2 and two molecules of GSH bind to each other through iron-sulfur clusters into a crystalline dimer, which becomes more sensitive to intracellular oxidative stress. When ROS is produced, the lens spatial configuration will be immediately reduced to two molecules of GSH and two molecules of Grx2, exerting antioxidant effects [13-14]. Grx2 is widely distributed in human organs, including the eye, where its expression has been found in the cornea, iris, lens, retina and optic nerve [15].

Mitochondria are closely associated with LEC metabolism, division, proliferation and differentiation and make a difference in normal physiological functions of the lens [16-17]. Grx2, an isoenzyme distributed in mitochondria, can directly protect lens proteins and enzymes, thereby maintaining lens transparency by regulating intracellular sulfhydryl groups. In recent years, KO mice have received considerable interest in research on genes and corresponding protein functions in China and abroad. In 2010, our research group in cooperation with the University of Nebraska observed and studied the occurrence of cataracts and the changes in biochemical indicators with age in *Grx1* KO mice as a model for the first time [18-19], and gained some experience in the establishment and breeding of *Grx1* KO mice. Wu *et al* [7] established the *Grx2* KO mouse model by the ES targeting method, and found that these mice developed lens opacity when aged 3 months. To further investigate the role of Grx2 in cataractogenesis, the group of Prof. Marjorie F. Lou at the University of Nebraska, USA generated the *Grx2* KO mice again, using the CRISPR/Cas9 system, in 2014 to investigate the association between cataract formation and mitochondrial function [20]. The CRISPR/Cas9 system has some advantages over the ES targeting method for KO, thereby shortening the construction cycle of KO mice, and exon 2 is knocked out by both the CRISPR/Cas9 system and ES targeting method to achieve *Grx2* KO. These two methods have no significant difference in their impact on the Grx2 protein expression level. Our research group continued our collaboration with Prof. Lou to construct B6J-*Grx2* KO mice, as well as B6J-*Grx2* KI mice, for the first time. Using the B6J-*Grx2* KO and B6J-*Grx2* KI mouse models, the role of Grx2 in cataractogenesis and the molecular mechanism by which Grx2 inhibits lens opacity were investigated.

In the present study, *Grx2* KO mice developed normally and no other systemic changes were observed, except for a slightly lower body mass than WT mice. A similar manifestationwas also found in *Grx1* (another member of the *Grx* family) KO mice [21]. Mitochondria are the main sites of energy metabolism. To understand whether *Grx2* KO mice had systemic abnormalities, histopathological analysis was performed on the metabolically active tissues (heart, brain, liver and muscle) of the mice. The results showed that there were no significant abnormalities in the organs of *Grx2* KO or *Grx2* KI mice, suggesting that neither *Grx2* deletion nor its up-regulation resulted in abnormal mitochondrial morphology or caused pathological changes in cells.

However, it was found that a small number of vacuoles appeared in the lens of *Grx2* KO mice from 3 months of age, and lens opacity developed rapidly at 4–5 months of age. By contrast, only a few vacuoles were found in the lens of WT mice of the same age, and the lens of *Grx2* KI mice remained transparent throughout the 5-month observation period. Without vessels and nerves, the lens primarily works through refraction and regulation. The lens of adult mice will rapidly grow and differentiate, and lens protein aggregation can be induced by a variety of endogenous and exogenous stress conditions, with oxidative stress being one of the major patterns of damage, ultimately leading to cataracts [22]. The dynamic balance between oxidative damage and antioxidant repair in the lens is responsible for maintaining lens transparency. In the present study, the lens ROS level of *Grx2* KO mice was analyzed and found to be far higher than that of WT mice. Moreover, the 8-OHdG level (a marker for oxidative DNA damage) was up-regulated in the lens of *Grx2* KO mice. The GSH system is a small molecule antioxidant in the lens, is a major player in the antioxidation-reduction balance in the lens, and is a key peptide in protecting protein sulfhydryl groups and GSSG homeostasis. In the present study, the GSH system in the lens of *Grx2* KO mice was investigated. The results revealed that the bcl-2, GSH and bax protein expression levels declined compared to those in WT mice, suggesting that as an isoenzyme of Grx1, Grx2 has a similar role in maintaining GSH/GSSG homeostasis.

In conclusion, *Grx2* KO and *Grx2* KI mouse models were established in this study, whereby it was found that *Grx2* KO could accelerate the occurrence of age-related cataracts, and it was confirmed that Grx2 is involved in the repair of cellular oxidative damage. The results demonstrated that Grx2 plays a protective role in the normal physiological function of the mouse lens, which can inhibit ROS production, down-regulate 8-OHdG expression, protect reduced-state GSH and reduce oxidized-state GSSG. Therefore, *Grx2* is of importance for the repair of lens oxidative damage and the maintenance of lens transparency.

Conflict of interest None declared.

Author contribution statement Guo Y: Experimental design, study implementation and manuscript writing; Guo CJ: Experimental operation, and manuscript revision; Zhang J: Paper revision; Ning XN: Data statistics; Yan H: Experimental design, manuscript revision and final drafting; Chen X: Animal feeding.

References

[1] Truscott RJ. Age-related nuclear cataract-oxidation is the key[J]. Exp Eye Res, 2005, 80(5): 709-725. DOI: 10.1016/j.exer.2004.12.007.

[2] Zhang J, Yan H. Establishment of Thioltransferase knockout mouse model and the function of thioltransferase in cataractogenesis[J]. Int Eye Sci, 2020, 20(3):420-425. DOI: 10.3980/j. issn.1672-5123.2020.3.05.

[3] Yan H, Harding JJ, Xing K, et al. Revival of glutathione reductase in human cataractous and clear lens extracts by thioredoxin and thioredoxin reductase, in conjunction with alpha-crystallin or thioltransferase[J]. Curr Eye Res, 2007, 32(5):455-463. DOI: 10.1080/ 02713680701257837.

[4] Yan H, Lou MF, Fernando MR, et al. Thioredoxin, thioredoxin reductase, and alpha-crystallin revive inactivated glyceraldehyde 3-phosphate dehydrogenase in human aged and cataract lens extracts[J]. Mol Vis, 2006, 12:1153-1159.

[5] Mailloux RJ, Jin X, Willmore WG. Redox regulation of mitochondrial function with emphasis on cysteine oxidation reactions[J]. Redox Biol, 2014, 2:123-139. DOI: 10.1016/j.redox.2013. 12.011.

[6] Mali P, Yang L, Esvelt KM, et al. RNA-guided human genome engineering via Cas9[J]. Science, 2013, 339(6121):823-826. DOI: 10.1126/science.1232033.

[7] Wu H, Yu Y, David L, et al. Glutaredoxin 2 (Grx2) gene deletion induces early onset of age-dependent cataracts in mice[J]. J Biol Chem, 2014, 289(52):36125-36139. DOI: 10.1074/ jbc.M114.620047.

[8] Hippenmeyer S, Youn YH, Moon HM, et al. Genetic mosaic dissection of Lis1 and Ndel1 in neuronal migration[J]. Neuron, 2010, 68(4):695-709. DOI: 10.1016/j.neuron.2010.09.027.

[9] Yan H, Guo Y, Zhang J, et al. Effect of carnosine, aminoguanidine, and aspirin drops on the prevention of cataracts in diabetic rats[J]. Mol Vis, 2008, 14:2282-2291.

[10] Mondal S, Kumar V, Singh SP. Phylogenetic distribution and structural analyses of cyanobacterial glutaredoxins (Grxs)[J/OL]. Comput Biol Chem, 2020, 84:107141[2022-03-10]. https://pubmed.ncbi.nlm.nih.gov/31839562/. DOI: 10.1016/j.compbiolchem.2019.107141.

[11] Fernandes AP, Holmgren A. Glutaredoxins: glutathione-dependent redox enzymes with functions far beyond a simple thioredoxin backup system[J]. Antioxid Redox Signal, 2004, 6(1):63-74. DOI: 10.1089/152308604771978354.

[12] Alloing G, Mandon K, Boncompagni E, et al. Involvement of glutaredoxin and thioredoxin systems in the nitrogen-fixing symbiosis between legumes and rhizobia[J/OL]. Antioxidants (Basel), 2018, 7(12):182[2022-03-10]. https://www.ncbi.nlm.nih.gov/pmc/articles/PMC6315 971/. DOI: 10.3390/antiox7120182.

[13] Mitra S, Elliott SJ. Oxidative disassembly of the [2Fe-2S] cluster of human Grx2 and redox regulation in the mitochondria[J]. Biochemistry, 2009, 48(18):3813-3815. DOI: 10.1021/ bi900112m.

[14] Askelöf P, Axelsson K, Eriksson S, et al. Mechanism of action of enzymes catalyzing thiol-disulfide interchange. Thioltransferases rather than transhydrogenases[J]. FEBS Lett, 1974, 38(3):263-267. DOI: 10.1016/0014-5793(74)80068-2.

[15] Pozzi L, Hodgson JA, Burrell AS, et al. Primate phylogenetic relationships and divergence dates inferred from complete mitochondrial genomes[J]. Mol Phylogenet Evol, 2014, 75:165-183. DOI: 10.1016/j.ympev.2014.02.023.

[16] Brennan L, Khoury J, Kantorow M. Parkin elimination of mitochondria is important for maintenance of lens epithelial cell ROS levels and survival upon oxidative stress exposure[J]. Biochim Biophys Acta Mol Basis Dis, 2017, 1863(1):21-32. DOI: 10.1016/j.bbadis.2016. 09.020.

[17] Zhou B, Zhao G, Zhu Y, et al. Protective effects of nicotinamide riboside on H2O2-induced oxidative damage in lens epithelial cells[J]. Curr Eye Res, 2021, 46(7):961-970. DOI: 10.1080/ 02713683.2020.1855662.

[18] Zhang J, Yan H, Löfgren S, et al. Ultraviolet radiation-induced cataract in mice: the effect of age and the potential biochemical mechanism[J]. Invest Ophthalmol Vis Sci, 2012, 53(11): 7276-7285. DOI: 10.1167/iovs.12-10482.

[19] Kronschläger M, Galichanin K, Ekström J, et al. Protective effect of the thioltransferase gene on in vivo UVR-300 nm-induced cataract[J]. Invest Ophthalmol Vis Sci, 2012, 53(1):248-252. DOI: 10.1167/iovs.11-8504.

[20] Zhang L, Yan Q, Liu JP, et al. Apoptosis: its functions and control in the ocular lens[J]. Curr Mol Med, 2010, 10(9):864-875. DOI: 10.2174/156652410793937741.

[21] Löfgren S, Fernando MR, Xing KY, et al. Effect of thioltransferase (glutaredoxin) deletion on cellular sensitivity to oxidative stress and cell proliferation in lens epithelial cells of thioltransferase knockout mouse[J]. Invest Ophthalmol Vis Sci, 2008, 49(10):4497-4505. DOI: 10.1167/iovs.07-1404.

[22] Ayala MN, Söderberg PG. Vitamin E can protect against ultraviolet radiation-induced cataract in albino rats[J]. Ophthalmic Res, 2004, 36(5):264-269. DOI: 10.1159/000081206.